Published online 8 September 2008 *Nucleic Acids Research, 2008, Vol. 36, No. 17* ***5713–5726***
doi:10.1093/nar/gkn572

Evidence for an inositol hexakisphosphate-dependent role for Ku in mammalian nonhomologous end joining that is independent of its role in the DNA-dependent protein kinase

Joyce C.Y. Cheung, Brenda Salerno and Les A. Hanakahi*

Department of Biochemistry and Molecular Biology, Johns Hopkins University, Bloomberg School of Public Health, Baltimore, MD 21205, USA

Received June 7, 2008; Revised August 22, 2008; Accepted August 23, 2008

ABSTRACT

Nonhomologous end-joining (NHEJ) is an important pathway for the repair of DNA double-strand breaks (DSBs) and plays a critical role in maintaining genomic stability in mammalian cells. While Ku70/80 (Ku) functions in NHEJ as part of the DNA-dependent protein kinase (DNA-PK), genetic evidence indicates that the role of Ku in NHEJ goes beyond its participation in DNA-PK. Inositol hexakisphosphate (IP_6) was previously found to stimulate NHEJ *in vitro* and Ku was identified as an IP_6-binding factor. Through mutational analysis, we identified a bipartite IP_6-binding site in Ku and generated IP_6-binding mutants that ranged from 1.22% to 58.48% of wild-type binding. Significantly, these Ku IP_6-binding mutants were impaired for participation in NHEJ *in vitro* and we observed a positive correlation between IP_6 binding and NHEJ. Ku IP_6-binding mutants were separation-of-function mutants that bound DNA and activated DNA-PK as well as wild-type Ku. Our observations identify a hitherto undefined IP_6-binding site in Ku and show that this interaction is important for DSB repair by NHEJ *in vitro*. Moreover, these data indicate that in addition to binding of exposed DNA termini and activation of DNA-PK, the Ku heterodimer plays a role in mammalian NHEJ that is regulated by binding of IP_6.

INTRODUCTION

Double-strand breaks (DSBs) in DNA represent a significant threat to viability and genomic integrity in all cells. In multicellular organisms, genomic instability arising from a DSB can lead to tumorigenesis, which makes the mechanisms of DSB repair of considerable interest. In late S or G2 phases of the cell cycle, DSBs can be repaired by homologous recombination. In G1 or early S phases of the cell cycle, the lack of sister chromatids dictates the use of the homology-independent DSB repair mechanism nonhomologous end-joining (NHEJ) (1). This is also the case for the terminally differentiated (G0) cells that constitute the majority of cells in multicellular organisms and makes NHEJ the more widely used DSB repair mechanism in humans (1). In addition to repair of spontaneous DSBs, NHEJ is also used to repair programmed DSBs that arise during rearrangement of the immunoglobulin loci through the processes of V(D)J and class switch recombination. Failure to repair these programed DSBs results in a lack of immunoglobulin production, and inappropriate repair of these unique DSBs has been linked to the establishment of lymphomas (2).

Genetic and biochemical analysis have identified several factors required for mammalian NHEJ. DNA ligase IV is directly responsible for restoration of the phosphodiester bond at the site of the DSB and forms a complex with the XRCC4 protein, which is required for ligase IV stability and is therefore required for NHEJ (1,2). XLF, also known as Cernunnos, is thought to bind XRCC4 to form a ligase IV/XRCC4/XLF complex, which is essential for NHEJ (3,4). Additionally, the Artemis nuclease has been shown to participate in this pathway and is thought to be required for processing of nonligatable ends (5).

The heterotrimeric DNA-dependent protein kinase (DNA-PK) is also required for NHEJ in mammals (6,7). Composed of the DNA-PK catalytic subunit (DNA-PKcs), a PI3K-related protein kinase, and the Ku70/80 heterodimer (Ku), this large protein complex assembles on exposed DNA termini to become an active protein kinase that is, in general, unique to vertebrates (6). Ku is composed of one 70 kDa (Ku70) subunit and one 86 kDa (Ku80) subunit. Heterodimerization of the Ku70 and Ku80 polypeptides results in a ring-shaped structure that can thread onto an exposed DNA end with both

*To whom correspondence should be addressed. Tel: +1 443 287 2515; Fax: +1 410 955 2926; Email: lhanakah@jhsph.edu

Ku70 and Ku80 polypeptides making contact with the DNA (8). This bipartite DNA-binding site, which is split between the Ku70 and Ku80 subunits, provides a molecular mechanism for the required heterodimerization and the observed structure-specific DNA end-binding activity of Ku (8). Interestingly, while Ku and DNA-PKcs are both required for DNA-PK activity, genetic experiments carried out in mice show that Ku and DNA-PKcs do not contribute equally to mammalian NHEJ. This is particularly evident in the formation of signal and coding joints during V(D)J recombination. DNA-PKcs deficiency in mice results in the inability to produce coding joints, while the ability to form signal joints is retained (6,7). In contrast, Ku-deficient mice fail to form both signal and coding joints (6,7). These observations indicate that the role of Ku in mammalian NHEJ extends beyond participation in DNA-PK.

We have shown that, in addition to activating DNA-PKcs, Ku binds the small, phosphate-rich molecule inositol hexakisphosphate (IP_6, Figure 1A), which we previously identified as a stimulatory factor in mammalian NHEJ (9,10). Subsequent publications demonstrated that binding of IP_6 by Ku did not change the ability of Ku to bind DNA or to assemble with DNA-PKcs to form DNA-PK (10,11). These data suggest that the role of IP_6 in mammalian NHEJ is tied to functions of Ku that are independent of DNA-PK. To determine if binding of IP_6 by Ku contributes to efficient NHEJ, we used mutational analysis to identify an IP_6-binding site in Ku. This mutational analysis revealed that the Ku IP_6-binding site, like its DNA-binding site, is bipartite and requires residues from both Ku70 and Ku80 subunits. IP_6-binding mutants of Ku were separation-of-function mutants that stimulated DNA-PK but showed reduced affinity for IP_6. These separation-of-function mutants were also impaired for complementation of NHEJ in Ku-depleted extracts, which demonstrates that formation of a Ku–IP_6 complex is important for efficient NHEJ *in vitro*. These data show that the role of Ku in mammalian NHEJ may be divided into DNA-PKcs-dependent and IP_6-dependent functions.

MATERIALS AND METHODS

Cloning and mutagenesis

Ku70 entry vector (pENTKu70) was created as follows: the human Ku70 cDNA (gift from S. West) was amplified using primers Ku70.N and Ku70.C and cloned into pCR® 8/GW/TOPO® (Invitrogen, Carlsbad, California). Ku80 entry vector (pREh_6Ku80) was created as follows: a

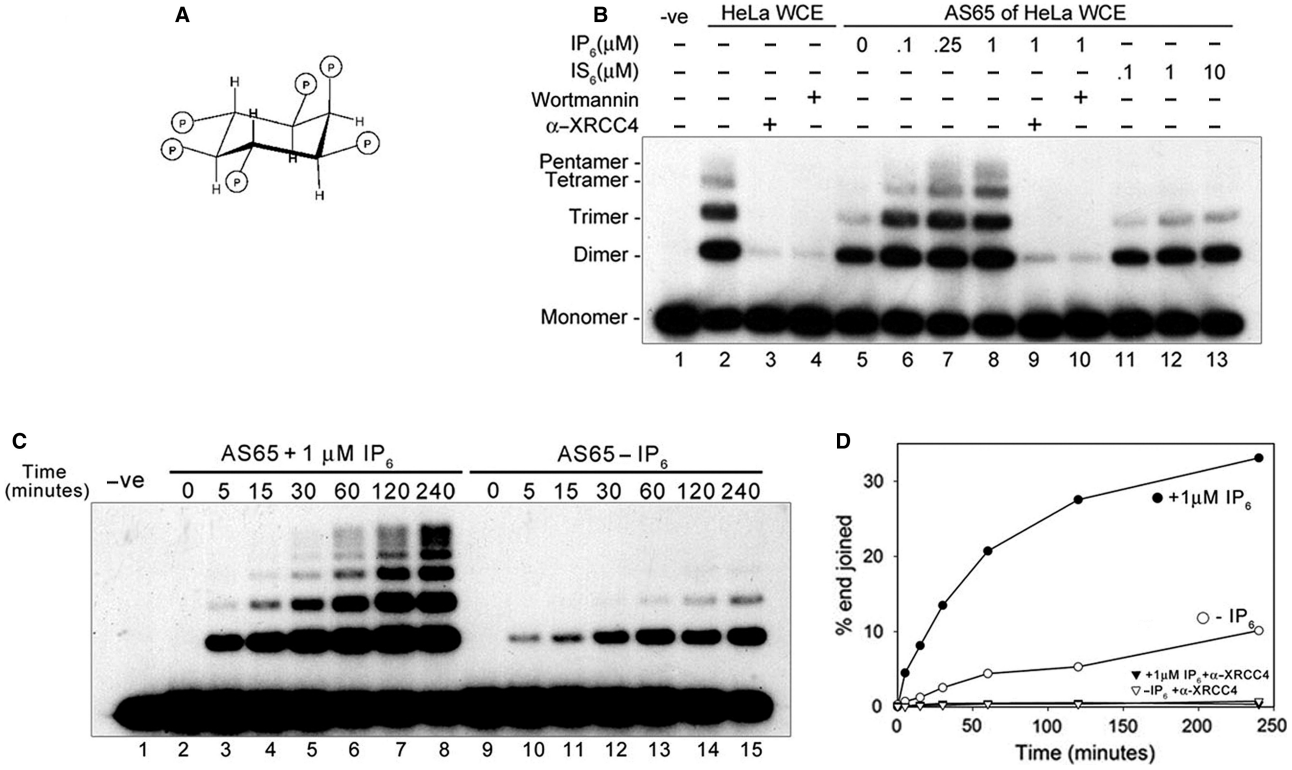

Figure 1. IP_6 is required for NHEJ *in vitro*. (**A**) Structure of IP_6. With D-myo-inositol as its base ring structure, IP_6 has one axial phosphate group (C-2), five phosphate groups in equatorial position and a molecular weight of 660 Da. (**B**) End-joining assays were carried out using 20 μg of HeLa WCE or AS65 as described in Materials and Methods section and complemented with IP_6 or IS_6. Treatment with *Wortmannin* (3 μM, lanes 4 and 10) and anti-XRCC4 antibodies (*α-XRCC4*, 1:250 dilution, lanes 3 and 9) demonstrate that the observed end joining is *bona fide* NHEJ. A −ve sign indicates no protein. Monomer, monomeric DNA substrate; dimer, trimer, etc., end-joined concatamers. (**C**) IP_6 increased the rate of NHEJ *in vitro*. AS65 (20 μg) was assayed for end joining as described in Materials and Methods section in the presence (left) or absence (right) of 1 μM IP_6 for the indicated time. (**D**) Quantification of C presented as percent of ends joined as a function of reaction time. Graph includes controls in which reactions were treated with anti-XRCC4 antibodies (1:250 dilution) to inhibit NHEJ (filled triangle, + IP_6 + α-XRCC4; open triangle, − IP_6 + α-XRCC4), which are not shown in (C).

his_6-tagged human Ku80 cDNA lacking the N-terminal five amino acids (gift from M. Lieber), was amplified using primers attB4Ku80N and attB1Ku80C, BP-recombined into pDONR^{TM}221 (Invitrogen) and the missing N-terminal five amino acids were replaced by site-directed mutagenesis (QuikChange II, Stratagene, La Jolla, CA) using N5Ku80s and its complement. Sequences for oligonucleotides used in cloning are provided in Supplementary Table 1. In pENTKu70 and pREh_6Ku80, lysine (K) residues were changed to alanines (A) by site-directed mutagenesis (QuikChange II, Stratagene) using oligonucleotides summarized in Supplementary Table 2. All sequences were confirmed by direct sequence analysis. Wild-type and K-to-A mutant cDNAs were LR-recombined into pDEST8 (Invitrogen) to create pBacuKu70, pBacuKu70DM, pBacuKu80, pBacuKu80DM and pBacuKu80TM.

Protein expression and purification

Baculoviruses were produced (BEVS, Invitrogen) and Sf-21 cells were coinfected at 10^6 cells/ml with Ku70 virus [Multiplicity Of Infection (M.O.I.) = 10] and h_6Ku80 virus (M.O.I. = 5) for 4 days. Purification was essentially as previously described (12). Briefly, cells were harvested by centrifugation (1000*g*, 15 min, 4°C), stored at −80°C then resuspended in 30 ml T Buffer (50 mM Tris pH 7.5, 0.4 M NH_4OAc, 0.3 M NaCl, 10% glycerol, 2 mM β-mercaptoethanol) with 0.2% NP-40 and 20 mM imidazole per 1 l original culture, lysed by homogenization (30 strokes, loose pestle) and PMSF was added to a final concentration of 1 mM. We determined that the high salt concentration of T Buffer was sufficient to remove >99% of prebound ^{3}H-IP_6 (data not shown). The resulting lysate was sonicated (8 × 15 s burst) and cellular debris was removed by centrifugation (10 000*g*, 10 min, 4°C). Binding to Talon (Clontech, Mountain View, CA) metal affinity resin was carried out in batch (1 h, 4°C), washed in batch with T Buffer, packed into a column and eluted T Buffer with 0.5 M imidazole. Eluted proteins were dialyzed into HepQ Buffer (50 mM Tris pH 7.5, 5% glycerol, 1 mM DTT and 1 mM sodium metabisulphite) with 50 mM NaCl, loaded onto a 5 ml Hi-trap heparin column (GE, USA) and eluted with a 50 mM to 1 M NaCl linear gradient in HepQ Buffer. Peak fractions were pooled, dialyzed against HepQ Buffer with 50 mM NaCl, loaded onto a 1 ml hi-trap Q column (GE) and eluted with a 50 mM to 1 M NaCl linear gradient in HepQ Buffer. Peak fractions were pooled, dialyzed against HepQ Buffer with 50 mM NaCl and 10% glycerol (4 h, 4°C), snap-frozen and stored at –80°C. Ku wild-type protein concentration was determined by A_{280} measurement. Ku mutant protein concentration was determined by Bradford assays using Ku wild-type as the protein standard.

Electrophoretic mobility shift assay

For examination of DNA binding by one Ku protein (8), 5′ GTTTTTAGTTTATTGGGCGCG 3′ was radiolabeled, annealed to 5′ CGCGCCCAGCTTTCCCAGCTA ATAAACTAAAAAC 3′ and gel purified. For examination of 1 and 2 Ku proteins bound to one double-stranded DNA (dsDNA), 5′ CTGAGAAAACTGTGCGTCTTCG CGGCAATTGAGAGGCATTCCATTCAC 3′ was radiolabeled, annealed to 5′ GTGAATGGAATGCCTCT CAATTGCCGCGAAGACGCACAGTTTTCTCAG 3′ and gel purified. Electrophoretic mobility shift assay (EMSA) was done essentially as previously described (12). Briefly, binding to duplex DNA was carried out in 10 µl reactions containing 50 mM Tris, pH 7.75, 100 mM KCl, 1 mM DTT, 5% glycerol, 100 µg/ml bovine serum albumin, 5 nM ^{32}P-labeled duplex DNA and recombinant Ku as stated for 30 min at room temperature. Complexes were resolved on 5% (29:1 acrylamide:bis) native PAGE in 0.5 × TBE at 2.5 V/min at room temperature. The gel was dried and subject to autoradiography. Unlabeled 1.8 kb dsDNA PCR fragment was used as dsDNA competitor. Unlabeled single-stranded DNA (ssDNA) competitor was 5′ GAAACAATAGGAAAG AAGTTTGAGGCGAGGCATATTGAAATATTCACT GA 3′. Quantification of EMSA: images were captured on a FLA-7000 Image Reader, processed using Multi Gauge V3.0 software (Fuji Film) as percentage of DNA bound by Ku = $B_{\text{shifted}}/(B_{\text{shifted}} + B_{\text{free DNA}})$, where B = band intensity.

DNA-PK assay

Ku-free DNA-PKcs was prepared from HeLa whole-cell extract (WCE) as follows: HeLa nuclear extract was prepared as previously described (13) and dialyzed against J Buffer (25 mM HEPES, pH 7.6, 2 mM $MgCl_2$, 0.5 mM EDTA, 20% glycerol, 1 mM DTT, 1 mM sodium metabisulphite and 0.2 mM PMSF) with 50 mM KCl. The extract was fractionated over the following columns: Q-sepharose Fast-flow (GE), on SP-sepharose Fast-flow (GE), Hi-Trap Heparin (GE) and dsDNA cellulose (Sigma, Montana, USA); all columns were run in J buffer and eluted with a 50 mM to 1 M linear KCl gradient. Following fractionation over dsDNA cellulose DNA-PK-containing fractions were pooled and the salt concentration adjusted to 0.6 M ammonium sulphate and fractionated on a Hi-Trap phenyl sepharose column (GE) with a linear gradient of 0.5–0 M ammonium sulphate in J Buffer with 50 mM KCl. Ku was detected by western blot analysis and found to be in the column flow through and 0.6 M ammonium sulphate wash fractions. Fractions containing DNA-PKcs, and lacking detectable Ku by western blot analysis, were pooled and dialyzed into J Buffer with 0.1 M KCl. DNA-PK was assayed using the SIGNAtect DNA-PK assay system (Promega, Madison, WI) according to manufacturer's specifications. A total of 0.463 pmol of partially purified DNA-PKcs was used in each kinase reaction.

IP_6 filter binding assay

^{3}H-IP_6 was purchased from Perkin Elmer, Waltham, Massachusett (custom order). Analytical strong anion exchange (SAX) HPLC was used to determine that 80% of ^{3}H counts were contained in ^{3}H-IP_6 and overall purity was 50% ^{3}H-IP_6. Attempts at preparative purification by SAX-HPLC were unsuccessful due to low specific activity and concentration of the ^{3}H-IP_6. Ku–^{3}H-IP_6 binding reactions (15 µl) were carried out in 20 mM HEPES

pH 7.6, 0.5 mM EDTA, 10% glycerol, 0.1 mg/ml BSA, 40 mM KOAc, 10 mM DTT with 10 mM KPO_4 pH 7.6 to provide an excess of phosphate to minimize nonspecific binding of ^{3}H-IP_6. The 46.3 nM ^{3}H-IP_6 and 500 nM Ku were found to produce maximum signal with minimum background. Reactions were incubated for 60 min. Nitrocellulose filter paper (Schleicher and Schuell, USA, BA85) was equilibrated with 20 mM HEPES pH 7.6, 0.5 mM EDTA, 10% glycerol, 10 mM KPO_4 pH 8.0, and 1.5 mM IP_6 after which the binding reaction was applied to the filter. Filters were washed 3 × with 20 mM HEPES, pH 7.6, 0.5 mM EDTA, 0.3 M NaCl then dried and ^{3}H-IP_6 was detected by scintillation counting. We determined that 100% of the Ku remained bound to the filter through this assay (data not shown). All solutions and steps were at 4°C. Competition assays (Figure 2A) were done by combining ^{3}H-IP_6 and unlabeled IP_6 or inositol hexasulphate (IS_6) before adding Ku to the reaction.

In vitro NHEJ analysis

HeLa WCE was prepared as previously described (14). To generate AS65, HeLa WCE before the final dialysis was subject to 65% ammonium sulphate precipitation and dialyzed against L Buffer (20 mM Tris pH 8.0, 0.1 M KOAc, 10% glycerol, 0.5 mM EDTA and 1 mM DTT) for 2–4 h. *In vitro* NHEJ assays were carried out essentially as previously described (9,14). Briefly, reactions (10 µl) were carried out in 50 mM HEPES pH 8.0, 40 mM KOAc, 0.5 mM $Mg(OAc)_2$, 1 mM ATP, 1 mM DTT, 0.1 mg/ml bovine serum albumin (BSA) and HindIII-linearized 5′-^{32}P-labeled pBluescript DNA (10 ng) with 20 µg of WCE, AS65 or Ku-depleted AS65. The potassium concentration was adjusted to 100 mM by the addition of KOAc. IP_6 (Calbiochem, Gibbstown, NJ, USA) and IS_6 (Sigma) were added as indicated. In complementation assays using Ku-depleted AS65, Ku was added at 180 nM. Neutralizing anti-XRCC4 antibodies (Serotec, Raleigh, NC) and wortmannin (Sigma) were used as indicated with no preincubation. Reactions were incubated for 2 h at 37°C, stopped by the addition of deproteinization solution (2 µl, 10 mg/ml Proteinase K, 50 mM EDTA, 0.1 M Tris pH 7.5, 2.5% SDS) and deproteinized for 30 min at 37°C. Products were separated by agarose gel electrophoresis (0.6%, TAE) and visualized by autoradiography. Quantification of end joining: images were captured on a FLA-7000 Image Reader, processed using Multi Gauge V3.0 software (Fuji Film) as percentage of ends joined = $\left[\sum(B)(Y/Y+1)/\sum(B)\right] \times 100$. B = Band intensity, Y = number of ends joined for that species and $Y+1$ is the number of 3 kb monomers in that band.

Ku-depleted extracts

Immunodepletions were carried out as previously described (12) with modifications. Briefly, monoclonal anti-Ku antibodies were conjugated to protein A sepharose beads (GE) overnight in NET-0.5 buffer (50 mM Tris pH 8.0, 0.15 M NaCl, 1 mM EDTA, 10% glycerol, and 0.5% NP-40) at 0.8 µg anti-Ku antibodies per 1 µl protein A sepharose resin. AS65 was adjusted to a final concentration of 0.5 M NaCl, added to the antibody-bound resin (100 µg AS65 µl resin) and incubated with gentle mixing (2 h, 4°C) after which the resin was removed by centrifugation. Immunodepletion was repeated three times and the Ku-depleted extract was dialyzed against L Buffer for 4 h and stored at −80°C.

Antibodies

Antibodies directed against XRCC4, DNA-PKcs and DNA Ligase IV (Serotec); Ku80 (Neomarkers); DNA ligases I and III (GeneTex) were used for western blot detection. Monoclonal anti-Ku70 (C-N3H10), anti-Ku80 (C-111) and anti-Ku70/80 (C-162) (Neomarkers) were used to immunodeplete Ku with similar success. Neutralizing anti-XRCC4 antiserum (Serotec) was used in NHEJ assays.

RESULTS

IP_6 is required for efficient NHEJ *in vitro*

We have previously described the identification of IP_6 as a stimulatory factor for mammalian NHEJ (9). These complementation studies were carried out using a phosphocellulose-bound (PC-C) fraction of human WCE (9).

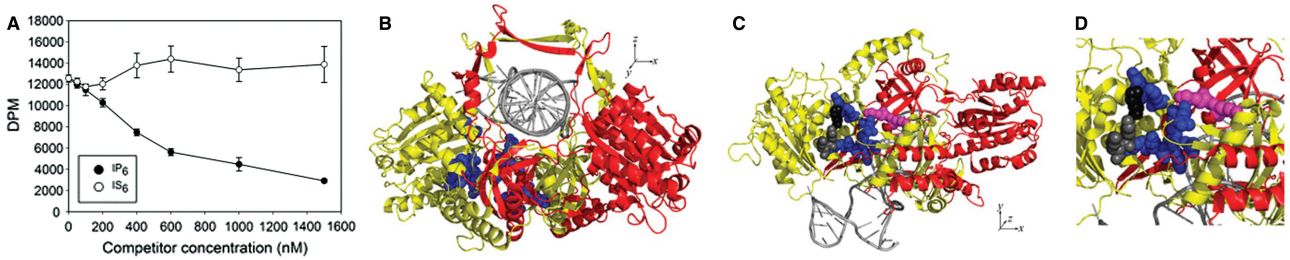

Figure 2. Binding of IP_6 by Ku. (**A**) Ku specifically binds to IP_6, but not IS_6. Filter binding assays were carried out as described in Materials and Methods section using 46.3 nM ^{3}H-IP_6 and 500 nM Ku in the presence of increasing amounts of unlabeled IP_6 or IS_6. Retained ^{3}H-IP_6 binding was measured as disintegration per minute (DPM). Values shown represent the mean of two independent experiments with each measurement made in triplicate ($N = 2$ and $n = 6$). Error bars show standard error. (**B**) Identification of a putative IP_6-binding site in Ku. The Ku70/80 ribbon structure is shown (PDB Accession No. 1JEY): Ku70 (red), Ku80 (yellow) and DNA (light gray). A cluster of conserved basic amino acids (blue space fill) is located near the Ku70/80 interface, away from the DNA-binding site and between the base of the Ku80 N-terminal α/β domain and the Ku70 central β-barrel domain. (**C**) Residues mutated in this study: 70DM—K357 K358 (pink space fill); 80DM—K238 K239 (dark gray space fill); and 80TM—K233 K238 K239 (K233 black space fill). Other basic amino acids that may be involved in Ku–IP_6 interaction but were not examined in this study are shown in blue. Bottom view of (B), which is rotated 90°. (**D**) Expanded view of (**C**).

We consistently observed that NHEJ catalyzed by PC-C in the presence of IP_6 was lower than that obtained with unfractionated WCE (data not shown), and reasoned that phosphocellulose fractionation must remove factors that contribute to the high levels of NHEJ catalyzed by WCE. To ensure that we were working with all of the factors necessary for efficient NHEJ *in vitro*, in the present study we used an IP_6-complementation assay based on WCE. Ammonium sulphate precipitation (65%) of WCE was used to generate a fraction (AS65) that contained the majority of proteins found in WCE and required IP_6 for efficient NHEJ *in vitro*. We observed that protein levels of NHEJ factors (Ku70, Ku80, DNA-PKcs, XRCC4 and ligase IV) were comparable between WCE and the AS65 fraction (Supplementary Figure 1). End joining catalyzed by the AS65 fraction, as characterized by the formation of concatamers, was greatly reduced when compared with end joining catalyzed by WCE (Figure 1B, compare lanes 2 and 5). Addition of IP_6 to the AS65 fraction restored concatamer formation to levels that recapitulated WCE-catalyzed end joining (Figure 1B, lanes 5–8). End joining catalyzed by WCE was unaffected by addition of IP_6 (data not shown), suggesting that sufficient IP_6 for maximum NHEJ was already present in these extracts.

To confirm that the observed IP_6-dependent DNA end joining was *bona fide* NHEJ, we treated reactions with the PI3-kinase inhibitor wortmannin, which inhibits DNA-PKcs activity (6), or with neutralizing anti-XRCC4 antibodies to assess requirements for DNA-PK and XRCC4, respectively. As shown in Figure 1B, treatment with either wortmannin or anti-XRCC4 antibodies inhibited ligation in WCE and in IP_6-complemented AS65. The requirement for IP_6 was specific, as IS_6, which has a negative-charge to mass ratio similar to that of IP_6, could not stimulate end joining *in vitro* (Figure 1B). Taken together, these data demonstrate that the IP_6-dependent ligation activity is classical, DNA-PK-dependent, XRCC4-dependent NHEJ and shows that IP_6 specifically stimulates NHEJ *in vitro*.

Time-course experiments showed that both the rate and extent of end joining by WCE and by the IP_6-complemented AS65 were similar (data not shown). In the absence of IP_6, however, the extent of concatamer formation was significantly reduced relative to similar reactions in the presence of IP_6 (Figure 1C). Control experiments showed that all of the end joining shown in Figure 1C was sensitive to neutralizing anti-XRCC4 antibodies and was therefore *bona fide* NHEJ (Figure 1D). These data show that ammonium sulphate precipitation can be used to generate a crude fraction (AS65) that catalyzes IP_6-dependent NHEJ that is as efficient as WCE and emphasize the importance of IP_6 in NHEJ *in vitro*.

Identification of an IP_6-binding site in Ku

Previously, we used gel filtration to show that Ku purified from HeLa cells was capable of binding IP_6 (10). To examine the IP_6-binding properties of Ku in greater detail, we developed a filter-binding assay and used competition analysis to assess the specificity of ^{3}H-IP_6-binding by wild-type recombinant Ku. To generate the data presented in Figure 2A, 46.3 nM ^{3}H-IP_6 was combined with increasing amounts of unlabeled IP_6 or IS_6 before adding Ku to the binding reactions. Wild-type recombinant Ku selectively bound IP_6 and did not bind IS_6 (Figure 2A), the charge-to-mass analog of IP_6 that failed to stimulate NHEJ in the PC-C (9) and AS65 (Figure 1B) fractions. Because binding reactions were carried out with 500 nM Ku, >500 nM unlabeled IP_6 was required to reduce bound ^{3}H-IP_6 by 50%. Impurities in the only commercially available source of ^{3}H-IP_6 limited the scope of possible experiments (see Materials and Methods section). Nonetheless, these data recapitulate the previously observed IP_6-binding by wild-type Ku (10,11) and demonstrate that the available ^{3}H-IP_6 can be used to assess specific IP_6 binding.

IP_6 is a six-carbon ring that is phosphorylated on all six carbons (Figure 1A). At physiological pH, IP_6 has a high negative charge-to-mass ratio, which predicts that electrostatic interactions play a large role in Ku IP_6 binding. In support of this prediction, we found that binding of IP_6 by Ku was very sensitive to the ionic strength of the binding reaction (data not shown). The chemical nature of IP_6 and the importance of charge-based interactions suggested that an IP_6-binding site would be composed of several positively charged amino acids. We had previously shown that binding of IP_6 by Ku affected the partial proteolysis patterns of both Ku70 and Ku80 subunits but did not affect DNA binding by Ku (10,11). Based on these observations, we predicted that the basic amino acids making up the Ku IP_6-binding site would be found on both subunits of Ku, and that these residues would not participate in DNA binding.

Through examination of the human Ku crystal structure (8), we identified a cluster of basic residues that might act as an IP_6-binding site. This putative IP_6-binding site is composed of lysines and arginines that do not participate in DNA binding and are located on both the Ku70 and Ku80 subunits. Multiple sequence alignments show that these residues are conserved between mammals (Tables 1 and 2), which suggested that these basic amino acids might play an important part in the biochemistry of Ku. The putative IP_6-binding site is located between the base of the Ku80 N-terminal α/β domain and the Ku70 central β-barrel domain (Figure 2B and C), which places it on the side of Ku that faces the continuous DNA strand, rather than toward the exposed DNA terminus.

To determine if this cluster of conserved, basic amino acids could act as an IP_6-binding site, we mutated groups of lysines to alanines to produce mutant Ku subunits with reduced positive charge in the putative IP_6-binding site. In the Ku80 subunit, lysines 238 and 239 (Figure 2D, dark gray spheres) were mutated to alanines to produce the double residue mutant $Ku80^{K238A/K239A}$, which we will refer to as 80^{DM}. Ku80 lysine 233 (Figure 2D, black sphere), which is less conserved than lysines 238 and 239 but located such that it may contribute to IP_6 binding, was also mutated to alanine to create the triple residue mutant $Ku80^{K233A/K238A/K239A}$, which we will refer to as 80^{TM}. In the Ku70 subunit, lysines 357 and 358 (Figure 2D, pink spheres) were mutated to alanines to create the double residue mutant $Ku70^{K357A/K358A}$, which we will refer to as 70^{DM}.

Table 1. Basic amino acids identified as candidate mediators of IP_6-binding by Ku—Ku70 sequence alignment

Human	Mouse	Rat	Hamster	Chicken	Xenopus	Zebrafish	*S. pombe*	*S. cerevisiae*
K 357	**K**	**K**	**K**	**K**	**K**	**K**	**K**	H
K 358	**K**	N	**K**	Q	**K**	L	P	Y
K 443	**K**	**K**	**K**	**K**	I	I	I	I
R 444	**R**	**R**	**R**	**R**	**R**	**R**	**R**	**R**
K 445	**K**	**K**	**K**	N	**K**	T	S	**K**

Accession numbers for the Ku70 amino acid sequences—Human, AAH12154; mouse, BAA28874; rat, AAH78718; hamster, AAB46854; chicken, BAA32018; Xenopus, NP_001082274; zebrafish, ABI54461; *S. pombe*, O94395; *S. cerevisiae*, P32807. Multiple sequence alignment was done using Clustal W (1.83). Amino acids that may participate in IP_6 binding by human Ku and the corresponding residues of other species as shown. Basic amino acids (lysines, K or arginines, R) are in bold. Lysine residues mutated in this study are underlined.

Table 2. Basic amino acids identified as candidate mediators of IP_6-binding by Ku—Ku80 sequence alignment

Human	Mouse	Rat	Hamster	Xenopus	Zebrafish	*S. pombe*	*S. cerevisiae*	Drosophila
R 44	**R**	**R**	**R**	**R**	R	H	N	D
R 232	**R**	Q	**R**	E	E	G	P	H
K 233	Q	Q	**R**	**R**	K	**R**	S	–
K 238	**K**	**K**	**K**	**K**	K	T	N	**K**
K 239	**K**	**K**	**K**	**K**	R	S	C	V
K 413	**K**	**K**	**K**	**K**	K	E	I	T
K 481	**K**	**K**	**K**	**K**	H	N	E	A

Accession numbers for the Ku80 amino acid sequences—Human, AAH95442; mouse, NP_033559; rat, NP_803154; hamster, 2211394A & AAC52664; Xenopus, BAA76954; zebrafish, NP_001017360; *S. pombe*, Q9HGM8; *S. cerevisiae*, Q04437; *D. melanogaster* (Drosophila), AAF63744. Multiple sequence alignment was done using Clustal W (1.83). Amino acids that may participate in IP_6 binding by human Ku and the corresponding residues of other species as shown. Basic amino acids (lysines, K or arginines, R) are in bold. Lysine residues mutated in this study are underlined.

To test the hypothesis that residues from Ku70 and Ku80 participate in IP_6 binding, we expressed each of the mutant Ku subunits with its wild-type partner ($Ku70/80^{DM}$, $Ku70/80^{TM}$ and $Ku70^{DM}/80$) to create single-subunit mutants of Ku. The control protein in which both subunits were wild-type (Ku70/80) was also expressed. All proteins described in this work were expressed by coinfection of insect cells with baculoviruses expressing individual Ku subunits and purified as described in Materials and Methods section. Cell lysis and immobilized metal affinity chelating chromatography were carried out in high salt to minimize copurification of IP_6. All of the recombinant proteins purified as heterodimers (Figure 3A and Supplementary Figure 2), which demonstrated that these mutations had little, if any, effect on the quaternary structure of the recombinant Ku proteins.

When the Ku single subunit lysine-to-alanine mutants were assayed for IP_6 binding we found that, for all three of the single-subunit mutant heterodimers tested, IP_6-binding was reduced relative to binding by wild-type Ku (Figure 3B). Limitations associated with the ^3H-IP_6 (see Materials and Methods section) prevented binding measurements at concentrations >500 nM, making binding constant measurements imprecise and restricting this analysis to relative binding by the recombinant Ku proteins.

At 463 nM ^3H-IP_6, the mutant Ku proteins showed a spectrum of IP_6-binding affinities at 58.5% of wild-type ($Ku70/80^{DM}$), 39.6% ($Ku70/80^{TM}$) and 17.4% of wild-type ($Ku70^{DM}/80$), which suggested that lysines in the IP_6-binding site did not participate equally in IP_6 binding. These results show that our mutational analysis has identified an IP_6-binding site in Ku and that residues from both Ku70 and Ku80 participate in IP_6 binding, which makes the IP_6-binding site of Ku bipartite. This mutational analysis has also produced mutant proteins with reduced affinities for IP_6.

IP_6-binding mutants of Ku are impaired for participation in NHEJ

To assess the ability of Ku IP_6-binding mutants to participate in NHEJ, we developed an assay system that required addition of both Ku and IP_6 for NHEJ *in vitro*. Starting with the AS65 fraction, which required addition of IP_6 for efficient NHEJ, high-salt conditions were used to disrupt Ku–protein and Ku–DNA interactions and selectively immunodepleted the abundant Ku protein (12). We confirmed that the Ku-depleted extracts contained no detectable levels of Ku70 or Ku80, but that the levels of other NHEJ factors were unaffected (Supplementary Figure 1). In the presence of IP_6, Ku-depleted AS65 had reduced end-joining activity relative to mock-depleted AS65, which was consistent with depletion of Ku (Figure 4A and Supplementary Figure 3). The end joining that was observed in the Ku-depleted AS65 was not sensitive to treatment with neutralizing anti-XRCC4 antibodies (Supplementary Figure 3A). We attribute this Ku-, XRCC4-independent concatamer formation to DNA ligases I and III, which had increased access to the DNA ends in the absence of Ku and were present in the Ku-depleted AS65 (Supplementary Figure 1). We conclude that the end joining observed in the Ku-depleted AS65 (Figure 4A, lane 3) does not represent background levels

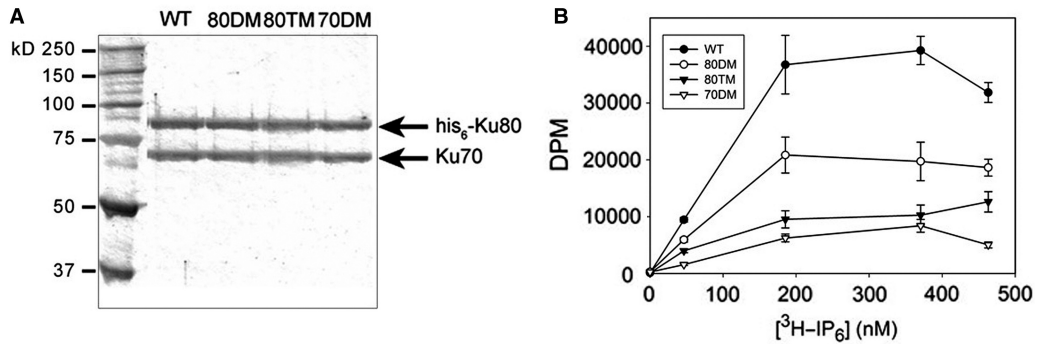

Figure 3. Characterization of single-subunit IP_6-binding mutants of Ku. (**A**) Purified Ku proteins used in this study. WT, wild-type Ku70/80; 80DM, Ku70/Ku80^{DM}; 80TM, Ku70/Ku80^{TM}; 70DM, Ku70^{DM}/Ku80. Mutant heterodimers were produced by coexpressing K-to-A mutant subunits with the corresponding wild-type subunit followed by purification as described in Materials and Methods section. A total of 0.5 µg total protein was resolved on 8% SDS–PAGE and silver stained. (**B**) Single-subunit Ku IP_6-binding mutants had decreased IP_6 binding relative to wild-type Ku. Filter binding assays were conducted as described in Materials and Methods section with 500 nM of recombinant Ku (wild-type or IP_6-binding mutants) and ^3H-IP_6 (as indicated). Values shown represent the mean of at least two independent experiments with each measurement made in triplicate (N = minimum of 2 and n = minimum of 6). Error bars show standard error. WT, wild-type Ku70/80; 80DM, Ku70/Ku80^{DM}; 80TM, Ku70/Ku80^{TM}; 70DM, Ku70^{DM}/Ku80.

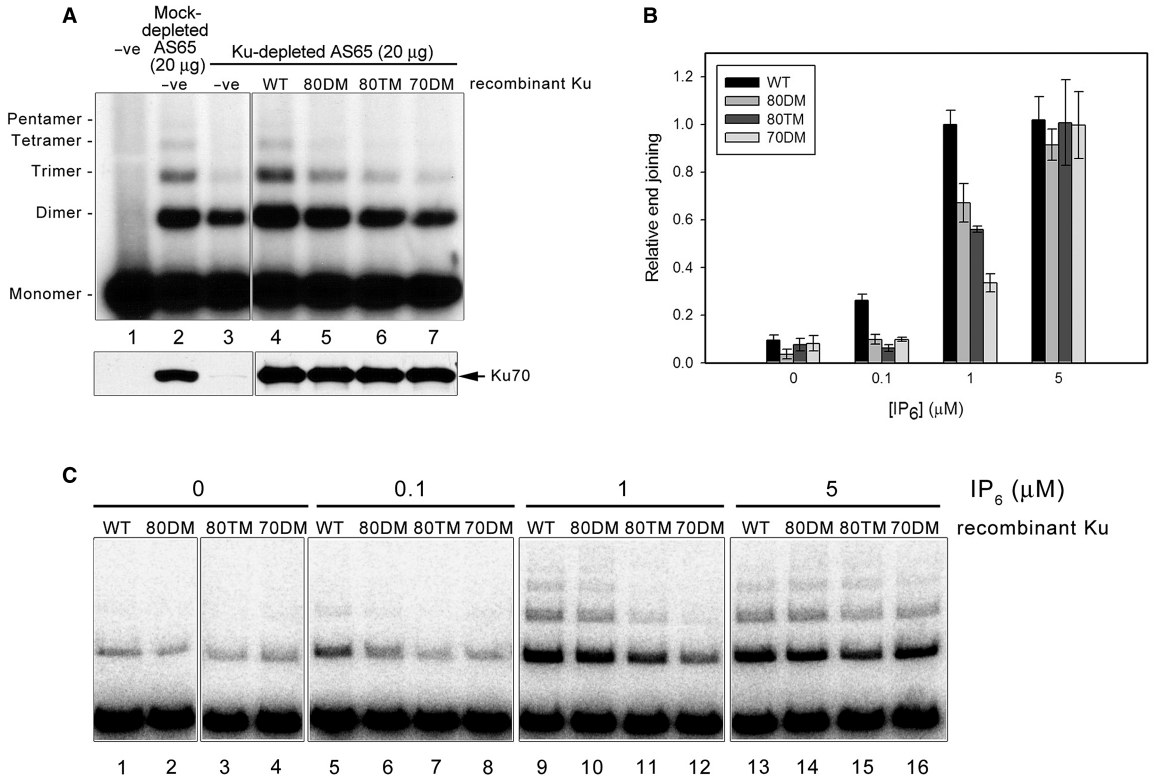

Figure 4. Single-subunit IP_6-binding mutants of Ku are impaired for complementation of end joining *in vitro*. (**A**) Top: Ku-depleted AS65 (20 µg) was complemented with 1 µM IP_6 and assayed for *in vitro* NHEJ as described in Materials and Methods section in the absence (lane 3) or presence (lanes 4–7) of recombinant Ku (180 nM, wild-type or IP_6-binding mutants). End joining observed in the absence of Ku (lane 3) was not sensitive to neutralizing anti-XRCC4 antibodies (Supplementary Figure 3A) and does not represent background levels of NHEJ. Mock-depleted AS65, anti-Ku antibodies omitted from immunodepletion. The negative sign indicates no protein. Top panel was assembled from lanes from a single autoradiogram. Bottom: anti-Ku70 Western blot shows the amount of endogenous Ku70 (lanes 2, 3) or recombinant Ku70 (lanes 4–7) present in the end-joining reactions (Top). Lane 2 shows the amount of endogenous Ku present in mock-depleted AS65 and lane 3 shows the extent of Ku depletion. Bottom panel was assembled from lanes from a single western blot. (**B**) Increasing IP_6 increases end joining in reactions complemented by single-subunit IP_6-binding mutants of Ku. Ku-depleted AS65 (20 µg) was complemented with 180 nM recombinant Ku (wild-type or IP_6-binding mutants) and IP_6 (as indicated), assayed for *in vitro* NHEJ, quantified as described in Materials and Methods section and normalized to the mean of end joining in the presence of wild-type Ku at 1 µM IP_6. Values shown represent the mean of two independent experiments with each measurement made in duplicate (N = 2 and n = 4). (**C**) Representative FLA-7000 Image Reader images used to generate (B). Figure was assembled from results from a single experiment.

of ligase IV-mediated NHEJ, but rather adventitious concatamer formation by ligase I or III.

Using western blot analysis to compare purified, recombinant, wild-type Ku of known concentration with the Ku in AS65 we determined that Ku was present at ~180 nM in the AS65 fraction (data not shown). Addition of 180 nM wild-type recombinant Ku to the Ku-depleted AS65 fraction restored both the Ku protein and IP_6-dependent end joining to levels observed with the mock-depleted control (Figure 4A and Supplementary Figure 3B). Complementation with single-subunit Ku IP_6-binding mutants under standard assay conditions (1 μM IP_6) failed to restore NHEJ activity to levels achieved with wild-type Ku (Figure 4). Ku-complemented, IP_6-dependent end joining was sensitive to treatment with wortmannin or anti-XRCC4 antibodies (Supplementary Figure 3B), indicating that complementation with IP_6 and recombinant Ku proteins restored *bona fide* NHEJ that was dependent upon both DNA-PKcs and XRCC4. End joining was not observed in Ku-complemented reactions that contained IS_6 (data not shown). These data demonstrate a link between formation of the Ku-IP_6 complex and NHEJ *in vitro*.

Positive correlation between Ku-IP_6 binding and end-joining activity *in vitro*

Direct binding studies with ^{3}H-IP_6 showed that IP_6 binding by the single-subunit mutant Ku proteins increased with increasing ^{3}H-IP_6 concentration (Figure 3B). Because the impaired NHEJ observed with the single-subunit Ku IP_6-binding mutants (Figure 4) showed a positive correlation with IP_6-binding activity (Figure 3B), we predicted that the single-subunit mutants should be able to carry out more efficient NHEJ at higher concentrations of IP_6. As shown in Figure 4, increases in IP_6 concentration resulted in increased NHEJ for all of the recombinant Ku proteins examined. Notably, at 5 μM IP_6, reactions complemented with single-subunit Ku IP_6-binding mutants were indistinguishable from those complemented with wild-type Ku (Figure 4C, lanes 13–16).

Time-course experiments showed that the rate of concatamer formation in reactions complemented with single-subunit Ku IP_6-binding mutants was reduced relative to that of wild-type Ku (Supplementary Figure 4). Furthermore, decreases in reaction rate correlated with relative decreases in IP_6-binding (Figure 3B). These data show striking similarities to the AS65 time course shown in Figure 1C. Specifically, end joining in reactions complemented with wild-type Ku and IP_6 (Supplementary Figure 4, top) reached a maximum near 120 min, as did the AS65 fraction in the presence of IP_6 (Figure 1C, left). Reactions complemented with single-subunit IP_6-binding mutant Ku proteins (Supplementary Figure 4) and reactions carried out with AS65 in the absence of IP_6 (Figure 1C, right) showed similar levels of end joining that continued to increase without reaching an apparent maximum, even after 4 h of incubation.

Control reactions showed that, in the absence of IP_6, NHEJ was minimal in reactions complemented with any of the Ku proteins used in this study (Figure 4C and Supplementary Figure 4). In the absence of Ku, however, concatamer formation was driven by factors that were insensitive to treatment with anti-XRCC4 antibodies (Supplementary Figure 3A) and was therefore not classical NHEJ. Concatamer formation that was independent of Ku, IP_6 and XRCC4 (Supplementary Figure 3A) may represent the *in vitro* activity associated with the recently described alternative or nonclassical end-joining pathway (15–19). We believe that concatamer formation observed in the absence of Ku did not represent background levels of ligase IV-catalyzed NHEJ, but represent a separate ligation mechanism that is normally inhibited in the presence of Ku.

Taken together, data presented in Figure 4 and Supplementary Figures 3 and 4 demonstrate that single-subunit lysine-to-alanine mutants of Ku are not impaired for participation in NHEJ but required higher concentrations of IP_6 to compensate for reductions in IP_6 affinity. Moreover, these data corroborate the observation that formation of a Ku–IP_6 complex is an important part of the NHEJ reaction.

Ku subunits act synergistically in IP_6 binding

Thus far, our data show that Ku heterodimers with mutations in either Ku70 or Ku80 had moderate reductions in IP_6 binding. This suggested that mutation of 2–3 lysines to alanines within individual subunits of Ku was insufficient to prevent binding of the highly charged IP_6 by the remaining positively charged residues. Figure 2 shows that residues from Ku70 and Ku80 may contribute to the overall positive charge within the bipartite IP_6-binding site of Ku and Figure 3 confirms the role of basic residues from both Ku70 and Ku80 in IP_6 binding. These data suggest that multiple lysine-to-alanine mutations from both Ku subunits are necessary to achieve a significant decrease in IP_6 binding. To address this possibility, we coinfected insect cells with viruses that expressed $Ku70^{DM}$ and either $Ku80^{DM}$ or $Ku80^{TM}$ to produce recombinant heterodimeric proteins in which both subunits carry mutations in the Ku IP_6-binding site: combinatorial mutants $Ku70^{DM}/80^{DM}$ and $Ku70^{DM}/80^{TM}$. Expression and purification of these combinatorial mutants showed that the mutant subunits formed stable heterodimers, indicating that the mutations did not significantly interfere with protein folding (Supplementary Figure 2B).

When the combinatorial mutants were assayed for IP_6 binding, we found that combining lysine-to-alanine mutations in Ku70 with those in Ku80 greatly reduced IP_6 binding to 3.78% ($Ku70^{DM}/80^{DM}$) or 1.22% ($Ku70^{DM}/80^{TM}$) of that observed with wild-type Ku (Figure 5). While IP_6 binding by the combinatorial IP_6-binding mutants was severely diminished, the remaining IP_6-binding activity was measurable and within the confidence limits of the IP_6-binding assay. Therefore, the combinatorial mutants had significantly reduced, but not abolished, IP_6-binding activity. The synergistic effects of combining $Ku70^{DM}$ with $Ku80^{DM}$ or $Ku80^{TM}$ further support the description of the Ku IP_6-binding site as

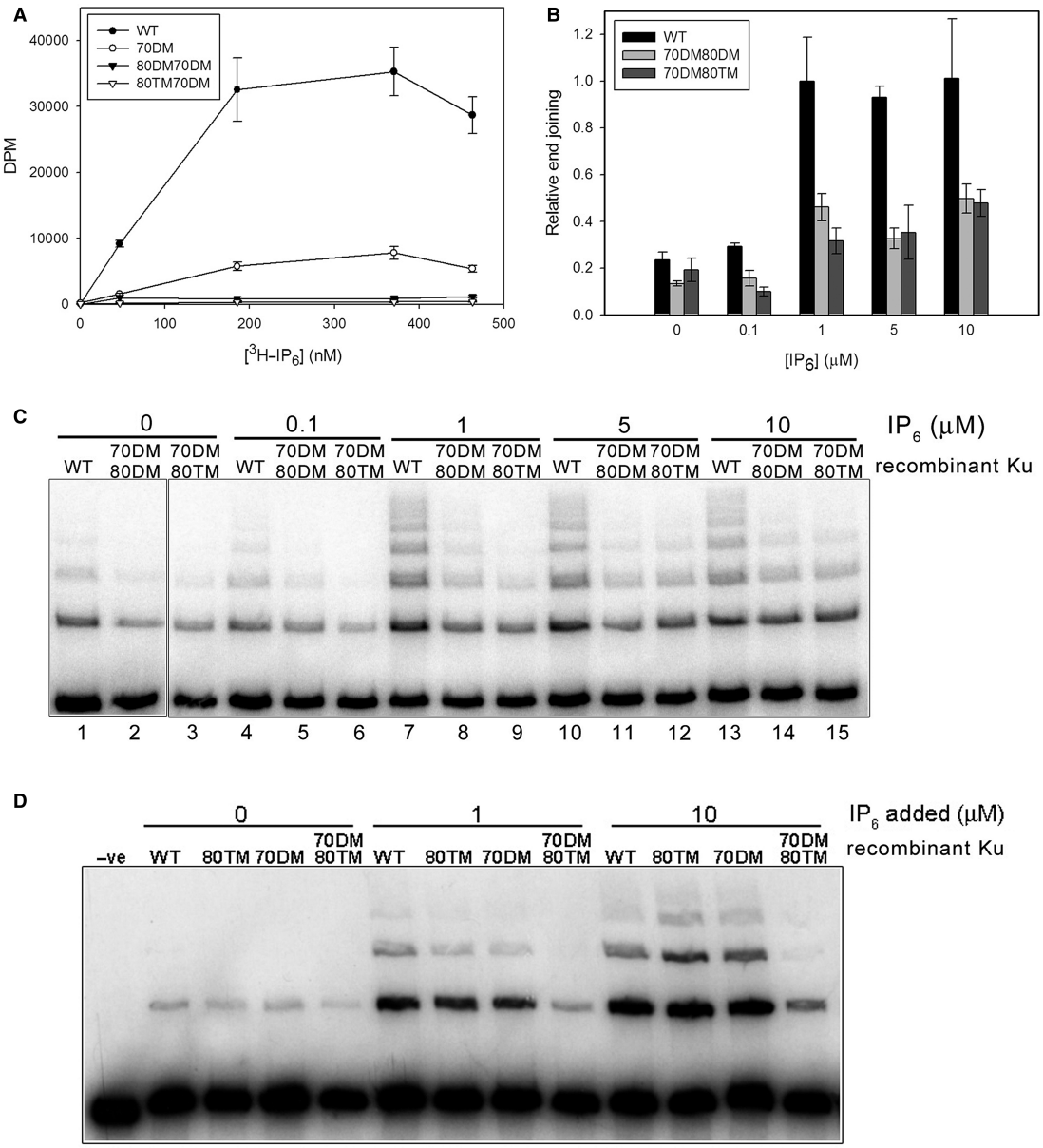

Figure 5. Combinatorial IP_6-binding mutants of Ku are impaired for complementation of end joining *in vitro*. (**A**) Combinatorial Ku IP_6-binding mutants had decreased IP_6 binding relative to wild-type Ku. Filter binding assays were conducted as described in Materials and Methods section with 500 nM of recombinant Ku (wild-type or IP_6-binding mutants) and ^3H-IP_6 (as indicated). Values shown represent the mean of at least two independent experiments with each measurement made in triplicate (N = minimum of 2 and n = minimum of 6). Error bars show standard error. WT, wild-type Ku70/80; 80DM70DM, $Ku70^{DM}/Ku80^{DM}$; 80TM70DM, $Ku70^{DM}/Ku80^{TM}$. (**B**) Increasing IP_6 does not increase end joining in reactions complemented by combinatorial IP_6-binding mutant Ku. Ku-depleted AS65 (20 μg) was complemented with 180 nM recombinant Ku (wild-type or IP_6-binding mutants) and IP_6 (as indicated), assayed for *in vitro* NHEJ, quantified as described in Materials and Methods section and normalized to the mean of end joining in the presence of wild-type Ku at 1 μM IP_6. Values shown represent the mean of two independent experiments (N = 2 and n = minimum of 3). (**C**) Representative FLA-7000 Image Reader images used to generate (B). Figure was assembled from results from a single experiment. (**D**) Comparison of end joining in reactions complemented with wild-type, single-subunit and combinatorial IP_6-binding mutants of Ku. Reactions were carried out as described for (B). WT, wild-type Ku70/80; 80TM, $Ku70/Ku80^{TM}$; 70DM, $Ku70^{DM}/Ku80$; 80TM70DM, $Ku70^{DM}/Ku80^{TM}$.

bipartite and demonstrate that we have correctly identified the IP_6-binding site of Ku.

Combinatorial IP_6-binding mutants of Ku are impaired for participation in NHEJ *in vitro*

To determine if the combinatorial IP_6-binding mutants of Ku were also impaired for participation in NHEJ *in vitro*, we complemented the Ku-depleted AS65 fraction with purified, recombinant wild-type and combinatorial IP_6-binding mutant Ku proteins (Figure 5B–D). As observed with the single-subunit IP_6-binding mutants, reactions complemented with $Ku70^{DM}/80^{TM}$ showed inefficient end joining in the absence of IP_6 (Figure 5B). Under standard assay conditions (1 μM IP_6), complementation of Ku-depleted AS65 with $Ku70/80^{TM}$ or $Ku70^{DM}/80$

resulted in detectable levels of end joining, while complementation with $Ku70^{DM}/80^{TM}$ did not. When the concentration of IP_6 was raised to 10 μM, end joining in reactions complemented with $Ku70/80^{TM}$ or $Ku70^{DM}/80$ was similar to that observed in reactions complemented with wild-type Ku, while complementation with $Ku70^{DM}/80^{TM}$ resulted in very little end joining. These data show that the combinatorial mutant $Ku70^{DM}/80^{TM}$, which was severely impaired for IP_6 binding, was also impaired for participation in NHEJ.

$Ku70^{DM}/80^{TM}$ retained only 1.22% of wild-type IP_6-binding activity and was severely impaired for participation in NHEJ, while $Ku70^{DM}/80^{DM}$ was less impaired for NHEJ and retained 3.78% of wild-type IP_6 binding. Figure 5C and D shows that the efficiency of end joining in reactions complemented with both combinatorial IP_6-binding mutants of Ku reached a maximum at 1 μM IP_6 and did not change with increasing IP_6 concentration. The IP_6-dependent end joining observed with the combinatorial mutants may be due to the low, but measurable, IP_6-bindng activity observed with $Ku70^{DM}/80^{DM}$ and $Ku70^{DM}/80^{TM}$. Alternately, while Ku depletion of the AS65 fraction used in the complementation experiments shown in Figure 5 was confirmed by western blot analysis, we cannot rule out the possibility that the IP_6-dependent end joining observed in Figure 5 may be due to residual endogenous Ku that was below the limit of western blot detection.

We found that variations in the preparation of the Ku-depleted AS65 fraction could lead to differences in the amount of end joining observed in Ku-complemented reactions. To directly compare the ability of combinatorial and single-subunit IP_6-binding mutants of Ku, we carried out the complementation reactions shown in Figure 5D. As previously observed, end joining in reactions complemented with wild-type recombinant Ku (WT) appeared to reach a maximum at 1 μM IP_6, with no further increase in NHEJ product formation observed at 10 μM IP_6. At 1 μM IP_6, end joining in reactions complemented with the single-subunit IP_6-binding mutants of Ku, $Ku70/80^{TM}$ (80TM) and $Ku70^{DM}/80$ (70DM), was reduced relative to reactions complemented with wild-type Ku. End joining in single-subunit IP_6-binding mutant complemented reactions increased with increasing IP_6 concentration and at 10 μM were indistinguishable from reactions complemented with wild-type Ku. In contrast, reactions complemented with the combinatorial mutant $Ku70^{DM}/80^{TM}$ (70DM80TM), which retained only 1.22% of wild-type IP_6-binding activity, produced very little end joining product under all IP_6 concentrations examined. The direct comparison presented in Figure 5D reinforces the correlation between Ku IP_6 binding and NHEJ *in vitro* and bipartite nature of the Ku IP_6-binding site.

Separation of DNA-PK activation and IP_6-binding properties of Ku

With the exception of IP_6 binding, the established functions of Ku in NHEJ are confined to its role in DNA-PK where Ku binds dsDNA ends (20,21) and contacts DNA-PKcs through the C-terminal domain of Ku80 to activate DNA-PKcs (22). It has been shown that binding of IP_6 by Ku does not affect the ability of Ku to bind DNA or to participate in DNA-PK assembly and that DNA-PK can assemble on DNA in a complex that incorporates IP_6 (10,11). Consistent with these reports, we show here that the IP_6-binding site of Ku is located away from sites of DNA and DNA-PKcs binding. Based on these findings, we predicted that the IP_6-binding mutants of Ku would be separation-of-function mutants that retain wild-type DNA-binding activity and the ability to activate DNA-PKcs.

First, we compared DNA binding by wild-type recombinant Ku, the single-subunit mutants $Ku70/80^{TM}$ and $Ku70^{DM}/80$ and the combinatorial mutants $Ku70^{DM}/80^{DM}$ and $Ku70^{DM}/80^{TM}$. The DNA used in this study, originally described by Walker *et al*. (8), uses a short piece of duplex DNA that can accommodate only one Ku protein. The termini of the synthetic duplex DNA permit directional loading of Ku from only one exposed end. Loading from the second terminus is prevented by the presence of an unpaired region, which can form a hammerhead structure (8). We used EMSA to assess DNA binding by wild-type and IP_6-binding mutants of Ku. A representative EMSA (Figure 6A) and the cumulative results of three experiments (Figure 6B) show that binding of a single Ku protein to DNA is comparable for all of the Ku proteins tested.

We also compared the DNA-end binding properties of the wild-type and IP_6-binding mutant Ku proteins by EMSA using a 48-bp duplex, which is large enough to permit loading of two Ku heterodimers. As shown by the representative EMSA data presented in Supplementary Figure 5, the dsDNA-binding activities of the three single subunit and the two combinatorial mutants IP_6-binding mutants were comparable to that of wild-type Ku. Small differences (1–5%) in DNA binding were observed between experiments, which we attribute to experimental variation. While cooperative binding by Ku has reported (20), we found that mutation of the Ku IP_6-binding site did not change the ability of Ku to form a two Ku:one DNA complex (Supplementary Figure 5). Additionally, the ability of Ku to specifically bind to exposed dsDNA termini was unaffected by mutation of the IP_6-binding site as neither single-stranded (Supplementary Figure 6) nor supercoiled circular DNA (data not shown) could compete for binding by recombinant wild-type or IP_6-binding mutant Ku proteins.

Having determined that the DNA-binding properties of Ku were unaffected by mutation of the IP_6-binding site, we went on to assess the ability of Ku IP_6-binding mutants to stimulate DNA-PKcs by comparing the ability of the wild-type and mutant Ku proteins to participate in phosphorylation of a p53 peptide substrate. DNA-PKcs is an active protein kinase in the absence of Ku (23,24). In this assay system, however, we did not observe significant phosphorylation of the p53 peptide substrate in reactions lacking Ku (Figure 6C and D). We saw no difference between the ability of recombinant wild-type Ku and the moderately impaired single-subunit IP_6-binding mutants of Ku to stimulate phosphorylation of a peptide substrate by DNA-PKcs (Figure 6C). Similarly, no difference was

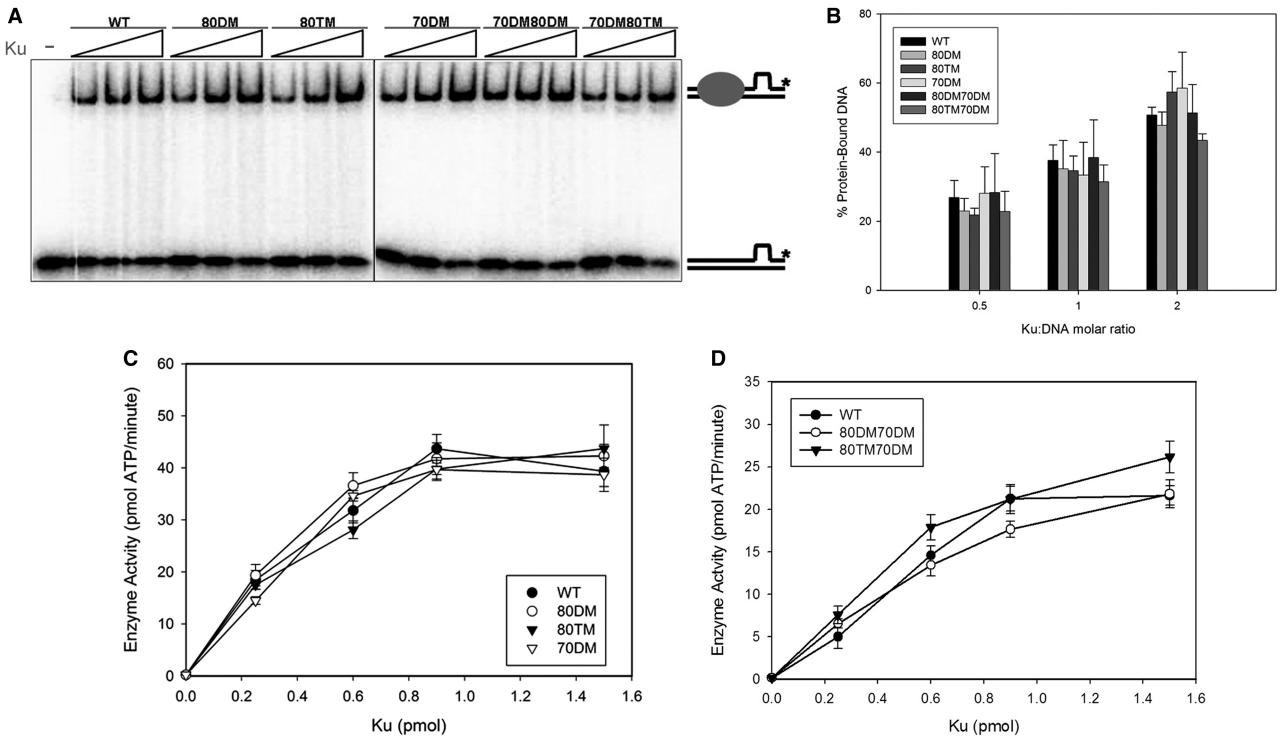

Figure 6. Separation of IP_6-binding- and DNA-PK-related functions of Ku. (**A**) dsDNA binding by IP_6-binding mutants of Ku. EMSA carried out with 5 nM of ^{32}P-end labeled dsDNA and recombinant Ku (as indicated) at 0, 2.5, 5 and 10 nM. Complexes were resolved on 5% native PAGE. Free dsDNA and dsDNA bound by 1 Ku protein as indicated. (**B**) DNA binding by wild-type and IP_6-binding mutants of Ku. EMSA was carried out as described for (A) with recombinant Ku proteins as indicated and quantified as described in Materials and Methods section and expressed as percentage of protein-bound DNA. Values shown represent the mean of three independent experiments. (**C**) Mutation of the IP_6-binding site did not affect activation of DNA-PKcs—analysis of single-subunit IP_6-binding mutants. DNA-PK assays were carried out as described using Ku-free DNA-PKcs (0.463 pmol) purified from HeLa cells and 0, 0.25, 0.6, 0.9 or 1.5 pmol recombinant Ku (wild-type or IP_6-binding mutants) and 10 μg/ml DNA. (**D**) Mutation of the IP_6-binding site did not affect activation of DNA-PKcs—analysis of combinatorial IP_6-binding mutants. DNA-PK assays were carried out as described for (B) with recombinant Ku proteins as indicated. Values shown for DNA-PK assays represent the mean of two independent experiments with each measurement made in triplicate ($N = 2$ and $n = 6$). Error bars show standard error. WT, wild-type Ku70/80; 80DM, Ku70/Ku80^{DM}; 80TM, Ku70/Ku80^{TM}; 70DM, Ku70^{DM}/Ku80; 80DM70DM, Ku70^{DM}/Ku80^{DM}; 80TM70DM, Ku70^{DM}/Ku80^{TM}.

observed between the ability of wild-type Ku and the more severely impaired combinatorial IP_6-binding mutants to stimulate DNA-PKcs (Figure 6D). We attribute the differences in DNA-PK activity between experiments (Figure 6C and D) to experimental variation.

Taken together, the data presented in Figure 6 show that IP_6-binding mutants of Ku with varying degrees of reduced affinity for IP_6 are not altered for DNA-end binding or for DNA-PKcs stimulation. Importantly, these data demonstrate that the IP_6-binding and NHEJ complementation experiments shown in Figures 3–5 were carried out with functionally equivalent amounts of recombinant Ku proteins. All of the IP_6-binding mutants of Ku represent separation-of-function mutants that highlight the role of Ku as an IP_6-binding protein, apart from its role in DNA-PK, in mammalian NHEJ.

DISCUSSION

We previously reported that Ku binds IP_6, which can act as a stimulator of NHEJ *in vitro*, and the formation of a Ku–IP_6 complex alters the protease accessibility of both Ku70 and Ku80 subunits (9,10). These results suggest that IP_6 binding may illicit changes in the structure of both Ku subunits. Here, we report the identification of a bipartite IP_6-binding site in Ku, which is comprised of residues from both Ku80 and Ku70 subunits and is located away from both the DNA-binding and DNA-PKcs-binding sites of Ku (8). Multiple sequence alignment showed that the IP_6-binding site of Ku, like the IP_6-binding site in the RNA editing enzyme ADAR2 (25), carries an overall positive charge and contains basic residues that are invariant among mammals. Distribution of positively charged amino acids that coordinate binding of IP_6 between Ku70 and Ku80 make the IP_6-binding site of Ku bipartite, as is the DNA-binding site (Figure 2). The mutational analysis presented here confirms the role of these basic residues in IP_6 binding and we have observed that combining lysine-to-alanine mutations in Ku70 with similar changes in Ku80 has a synergistic effect on reducing IP_6 binding. These basic amino acids do not appear to be found in the yeasts *Saccharomyces cerevisiae* or *Schizosaccharomyces pombe* (Tables 1 and 2), which is in keeping with the observation that yKu70/80 failed to interact with IP_6 (10). Like DNA-PKcs, which has no homolog in yeast, the binding of IP_6 by Ku and modulation of NHEJ by IP_6 are apparently unique to mammalian NHEJ.

Separation-of-function mutants of Ku generated in this study confirm the functionality of the bipartite IP_6-binding site identified in human Ku and highlight the importance of a Ku–IP_6 complex in mammalian NHEJ. These mutants represent a spectrum of reduced affinities for IP_6, while retaining the ability to heterodimerize, bind dsDNA and stimulate DNA-PK for phosphorylation of a commonly used p53 peptide substrate. Most significantly, these Ku IP_6-binding mutants are impaired for their ability to participate in NHEJ *in vitro*. We observed a correlation between IP_6 affinity and NHEJ activity, and found that single-subunit IP_6-binding mutants of Ku could effectively stimulate NHEJ when IP_6 levels were appropriately increased. These data show that the single-subunit IP_6-binding mutants of Ku are not absolutely deficient for participation in NHEJ, but simply impaired for IP_6 binding, which is necessary for efficient NHEJ *in vitro*.

Ku interacts with DNA and DNA-PKcs using nonoverlapping binding sites that permit formation of the active DNA-PK. We show here that the IP_6-binding site of Ku is located away from the sites of both DNA binding and DNA-PKcs binding, which is in structural agreement with formation of a DNA/DNA-PKcs/Ku–IP_6 complex. We had previously observed that direct addition of IP_6 to DNA-PK reactions had no effect on protein kinase activity, the requirement for DNA or inhibition by wortmannin (L.A.H. and West, unpublished observation). Additionally, a Ku heterodimer composed of a wild type, full-length Ku70 and a C-terminally truncated Ku80, which lacked the DNA-PKcs binding site of Ku, bound IP_6 as well, if not better, than wild-type, full-length Ku70/80 (10). In light of this history, it is not surprising that stimulation of DNA-PK by wild-type Ku and IP_6-binding mutants of Ku are comparable. Taken together, these findings demonstrate that binding of IP_6 by Ku does not affect DNA binding by Ku (11), assembly of DNA-PK (10,11) or DNA-PK activity.

Genetic analysis of mammalian V(D)J recombination suggests that the role of Ku is not restricted to its participation in DNA-PK. As referenced earlier, Ku deficiencies do not phenocopy a DNA-PKcs deficiency. Specifically, Ku70- and Ku80-deficient mice fail to produce signal and coding joints, while in DNA-PKcs-deficient animals signal joint formation is retained (6,7). Our findings indicate that binding of IP_6 and stimulation of DNA-PK are independent functions of Ku. Furthermore, these data imply that Ku plays a DNA-PK-independent role in mammalian NHEJ that is regulated by binding of IP_6.

Inositol polyphosphates as regulators of nuclear processes

The inositol phosphates (InsPs) have been shown to regulate a number of important nuclear functions, including ATP-dependent chromatin remodeling (26), telomere length maintenance (27,28), adenosine deamination in RNA editing (25) and mRNA export (29,30). InsPs can directly participate in these pathways, as typified by the RNA editing adenosine deaminase ADAR2 where binding of IP_6 by ADAR2 is required for ADAR2 catalytic activity (25). There is also evidence for indirect participation of InsPs, as is the case with stimulation of Dpn5 ATPase activity by the Gle1–IP_6 complex in mRNA export (30). Given that Ku possesses no known enzymatic activities, it is most likely that IP_6 acts indirectly to stimulate NHEJ by modulating interactions between Ku and other nuclear factors.

Studies of InsP metabolism have found that InsP homeostasis is highly regulated and that intracellular concentrations of IP_6, reported to be in the low micromolar range in mammalian cells, are relatively stable (31). Given these observations, how can a molecule like IP_6 play a regulatory role in such a wide variety of nuclear processes? The current hypothesis suggests that the InsPs, like Ca^{2+}, may exist in subcellular pools that can be independently regulated (32). There is evidence that InsP metabolism, and therefore the abundance of specific InsP species, can be modulated by G protein activation (31), which could certainly link the InsPs to the cell signaling network. The recent identification of IP_6 in the crystal structure of the Arabidopsis TIR1 ubiquitin ligase, which participates in the regulation of plant growth through auxin hormone signaling, highlights the connection between signaling and InsP metabolism (33).

Possible roles for IP_6 in NHEJ

While the role of the Ku–IP_6 complex in NHEJ remains elusive, findings presented here suggest three possible mechanisms for indirect regulation of NHEJ by IP_6. First, recent publications have shown that multiple low-affinity protein–protein interactions exist between the DNA-PK and XRCC4/ligase IV/XLF complexes and that these apparently weak or transient interactions are stabilized in the presence of DNA. In particular, Ku70 has been shown to make direct contact with ligase IV and with XRCC4 (34–36). It is worth noting that the experiments that defined these interactions between NHEJ factors were carried out in cell-free extracts, which presumably contain IP_6 (34). These findings suggest the hypothesis that binding of IP_6 by Ku might influence the stability of protein–protein interactions that connect the NHEJ apparatus, which results in the observed stimulation of NHEJ. We believe this to be the most likely mechanism of IP_6 stimulation of mammalian NHEJ and we are currently investigating the effects of IP_6 on the stability of Ku-XRCC4/ligase IV/XLF interactions.

Second, although we show that formation of a Ku–IP_6 complex does not affect any aspect of DNA-PK phosphorylation of a p53 peptide substrate, we cannot rule out the possibility that binding of IP_6 by Ku could affect substrate selection by DNA-PK, which may influence NHEJ. Published work on the role of DNA-PK autophosphorylation in NHEJ (37,38) make modulation of DNA-PK substrate selection a plausible, if unlikely, mechanism for stimulation of NHEJ by IP_6.

Finally, the IP_6-binding site of Ku is located on the surface of Ku that faces the continuous DNA strand (8), which raises the possibility that IP_6 may regulate interactions between Ku and DNA-binding factors that do not act at the exposed DNA end. Previous findings have shown that nucleosome assembly and linker histone H1 binding inhibits NHEJ *in vitro* (39), and that Ku is capable

of displacing assembled nucleosomes and histone H1 (40). Binding of IP_6 to the side of Ku that faces the continuing DNA strand may affect interactions between Ku and DNA-binding proteins to increase NHEJ efficiency by stimulating eviction of bound proteins from the region of the DSB.

SUPPLEMENTARY DATA

Supplementary Data are available at NAR Online.

ACKNOWLEDGEMENTS

We are grateful to Randy Bryant whose careful reading of the article and thoughtful comments made a significant impact on the presentation of this work. We thank Steve Desderio, William Wright, Timra Gilson, Sumithra Jayaram and B.T. Rantipole for many thoughtful discussions; and Rashna Bhandari and Solomon Snyder for assistance with purchasing and analyzing the ^3H-IP_6. We also thank Ronald Stamper and Claire Hauer for effort contributed to developing the NHEJ IP_6 complementation assay.

FUNDING

National Institutes of Health (GM072114 to B.S., GM070639 to L.A.H); Johns Hopkins University, Bloomberg School of Public Health, Faculty Innovation Fund to L.A.H; National Institutes of Health, National Center for Research Resources (U42 RR05991) for HeLa cells obtained from the National Cell Culture Center (Minneapolis, MN). Funding for open access charge: National Institutes of Health, GM00639.

Conflict of interest statement. None declared.

REFERENCES

1. Sonoda,E., Hochegger,H., Saberi,A., Taniguchi,Y. and Takeda,S. (2006) Differential usage of non-homologous end-joining and homologous recombination in double strand break repair. *DNA Repair*, **5**, 1021–1029.
2. Lieber,M.R., Ma,Y., Pannicke,U. and Schwarz,K. (2004) The mechanism of vertebrate nonhomologous DNA end joining and its role in V(D)J recombination. *DNA Repair*, **3**, 817–826.
3. Ahnesorg,P., Smith,P. and Jackson,S.P. (2006) XLF interacts with the XRCC4-DNA ligase IV complex to promote DNA nonhomologous end-joining. *Cell*, **124**, 301–313.
4. Buck,D., Malivert,L., de Chasseval,R., Barraud,A., Fondaneche,M.C., Sanal,O., Plebani,A., Stephan,J.L., Hufnagel,M., le Deist,F. *et al*. (2006) Cernunnos, a novel nonhomologous end-joining factor, is mutated in human immunodeficiency with microcephaly. *Cell*, **124**, 287–299.
5. Lobrich,M. and Jeggo,P.A. (2005) Harmonising the response to DSBs: a new string in the ATM bow. *DNA Repair*, **4**, 749–759.
6. Smith,G.C. and Jackson,S.P. (1999) The DNA-dependent protein kinase. *Genes Dev.*, **13**, 916–934.
7. Collis,S.J., DeWeese,T.L., Jeggo,P.A. and Parker,A.R. (2005) The life and death of DNA-PK. *Oncogene*, **24**, 949–961.
8. Walker,J.R., Corpina,R.A. and Goldberg,J. (2001) Structure of the Ku heterodimer bound to DNA and its implications for double-strand break repair. *Nature*, **412**, 607–614.
9. Hanakahi,L.A., Bartlet-Jones,M., Chappell,C., Pappin,D. and West,S.C. (2000) Binding of inositol phosphate to DNA-PK and stimulation of double-strand break repair. *Cell*, **102**, 721–729.
10. Hanakahi,L.A. and West,S.C. (2002) Specific interaction of IP6 with human Ku70/80, the DNA-binding subunit of DNA-PK. *EMBO J.*, **21**, 2038–2044.
11. Ma,Y.M. and Lieber,M.R. (2002) Binding of inositol hexakisphosphate (IP6) to Ku but not to DNA-PKcs. *J. Biol. Chem.*, **277**, 10756–10759.
12. Hanakahi,L.A. (2007) 2-Step purification of the Ku DNA repair protein expressed in Escherichia coli. *Protein Expr. Purif.*, **52**, 139–145.
13. Dignam,J.D., Lebovitz,R.M. and Roeder,R.G. (1983) Accurate transcription initiation by RNA polymerase II in a soluble extract from isolated mammalian nuclei. *Nucleic Acids Res.*, **11**, 1475–1489.
14. Baumann,P. and West,S.C. (1998) DNA end-joining catalyzed by human cell-free extracts. *Proc. Natl Acad. Sci. USA*, **95**, 14066–14070.
15. Corneo,B., Wendland,R.L., Deriano,L., Cui,X., Klein,I.A., Wong,S.Y., Arnal,S., Holub,A.J., Weller,G.R., Pancake,B.A. *et al*. (2007) Rag mutations reveal robust alternative end joining. *Nature*, **449**, 483–486.
16. Yan,C.T., Boboila,C., Souza,E.K., Franco,S., Hickernell,T.R., Murphy,M., Gumaste,S., Geyer,M., Zarrin,A.A., Manis,J.P. *et al*. (2007) IgH class switching and translocations use a robust non-classical end-joining pathway. *Nature*, **449**, 478–482.
17. Weinstock,D.M., Brunet,E. and Jasin,M. (2007) Formation of NHEJ-derived reciprocal chromosomal translocations does not require Ku70. *Nat. Cell Biol.*, **9**, 978–981.
18. Windhofer,F., Wu,W. and Iliakis,G. (2007) Low levels of DNA ligases III and IV sufficient for effective NHEJ. *J. Cell Physiol.*, **213**, 475–483.
19. Windhofer,F., Wu,W., Wang,M., Singh,S.K., Saha,J., Rosidi,B. and Iliakis,G. (2007) Marked dependence on growth state of backup pathways of NHEJ. *Int. J. Radiat. Oncol. Biol. Phys.*, **68**, 1462–1470.
20. Ma,Y.M. and Lieber,M.R. (2001) DNA length-dependent cooperative interactions in the binding of Ku to DNA. *Biochemistry*, **40**, 9638–9646.
21. Arosio,D., Cui,S., Ortega,C., Chovanec,M., Di Marco,S., Baldini,G., Falaschi,A. and Vindigni,A. (2002) Studies on the mode of Ku interaction with DNA. *J. Biol. Chem.*, **277**, 9741–9748.
22. Gell,D. and Jackson,S.P. (1999) Mapping of protein-protein interactions within the DNA-dependent protein kinase complex. *Nucleic Acids Res.*, **27**, 3494–3502.
23. Carter,T., Vancurova,I., Sun,I., Lou,W. and DeLeon,S. (1990) A DNA-activated protein kinase from HeLa cell nuclei. *Mol. Cell Biol.*, **10**, 6460–6471.
24. Lees-Miller,S.P., Chen,Y.R. and Anderson,C.W. (1990) Human cells contain a DNA-activated protein kinase that phosphorylates simian virus 40 T antigen, mouse p53, and the human Ku autoantigen. *Mol. Cell Biol.*, **10**, 6472–6481.
25. Macbeth,M.R., Schubert,H.L., Vandemark,A.P., Lingam,A.T., Hill,C.P. and Bass,B.L. (2005) Inositol hexakisphosphate is bound in the ADAR2 core and required for RNA editing. *Science*, **309**, 1534–1539.
26. Shen,X., Xiao,H., Ranallo,R., Wu,W.H. and Wu,C. (2003) Modulation of ATP-dependent chromatin-remodeling complexes by inositol polyphosphates. *Science*, **299**, 112–114.
27. York,S.J., Armbruster,B.N., Greenwell,P., Petes,T.D. and York,J.D. (2005) Inositol diphosphate signaling regulates telomere length. *J. Biol. Chem.*, **280**, 4264–4269.
28. York,J.D., Guo,S., Odom,A.R., Spiegelberg,B.D. and Stolz,L.E. (2001) An expanded view of inositol signaling. *Adv. Enzyme Regul.*, **41**, 57–71.
29. York,J.D., Odom,A.R., Murphy,R., Ives,E.B. and Wente,S.R. (1999) A phospholipase C-dependent inositol polyphosphate kinase pathway required for efficient messenger RNA export. *Science*, **285**, 96–100.
30. Weirich,C.S., Erzberger,J.P., Flick,J.S., Berger,J.M., Thorner,J. and Weis,K. (2006) Activation of the DExD/H-box protein Dbp5 by the nuclear-pore protein Gle1 and its coactivator InsP6 is required for mRNA export. *Nat. Cell Biol.*, **8**, 668–676.

31. Otto,J.C., Kelly,P., Chiou,S.T. and York,J.D. (2007) Alterations in an inositol phosphate code through synergistic activation of a G protein and inositol phosphate kinases. *Proc. Natl Acad. Sci. USA*., **104**, 15653–8
32. Shears,S.B. (2001) Assessing the omnipotence of inositol hexakisphosphate. *Cell Signal*, **13**, 151–158.
33. Tan,X., Calderon-Villalobos,L.I., Sharon,M., Zheng,C., Robinson,C.V., Estelle,M. and Zheng,N. (2007) Mechanism of auxin perception by the TIR1 ubiquitin ligase. *Nature*, **446**, 640–645.
34. Costantini,S., Woodbine,L., Andreoli,L., Jeggo,P.A. and Vindigni,A. (2007) Interaction of the Ku heterodimer with the DNA ligase IV/Xrcc4 complex and its regulation by DNA-PK. *DNA Repair*, **6**, 712–722.
35. Mari,P.O., Florea,B.I., Persengiev,S.P., Verkaik,N.S., Bruggenwirth,H.T., Modesti,M., Giglia-Mari,G., Bezstarosti,K., Demmers,J.A., Luider,T.M. *et al*. (2006) Dynamic assembly of end-joining complexes requires interaction between Ku70/80 and XRCC4. *Proc. Natl Acad. Sci. USA*, **103**, 18597–18602.
36. Hsu,H.L., Yannone,S.M. and Chen,D.J. (2002) Defining interactions between DNA-PK and ligase IV/XRCC4. *DNA Repair*, **1**, 225–235.
37. Ding,Q., Reddy,Y.V., Wang,W., Woods,T., Douglas,P., Ramsden,D.A., Lees-Miller,S.P. and Meek,K. (2003) Autophosphorylation of the catalytic subunit of the DNA-dependent protein kinase is required for efficient end processing during DNA double-strand break repair. *Mol. Cell Biol*., **23**, 5836–5848.
38. Chan,D.W., Chen,B.P., Prithivirajsingh,S., Kurimasa,A., Story,M.D., Qin,J. and Chen,D.J. (2002) Autophosphorylation of the DNA-dependent protein kinase catalytic subunit is required for rejoining of DNA double-strand breaks. *Genes Dev*., **16**, 2333–2338.
39. Kysela,B., Chovanec,M. and Jeggo,P.A. (2005) Phosphorylation of linker histones by DNA-dependent protein kinase is required for DNA ligase IV-dependent ligation in the presence of histone H1. *Proc. Natl Acad. Sci. USA*, **102**, 1877–1882.
40. Roberts,S.A. and Ramsden,D.A. (2007) Loading of the nonhomologous end joining factor, Ku, on protein-occluded DNA ends. *J. Biol. Chem*., **282**, 10605–10613.